Development of a simple, open-source hurricane wind risk model for Bermuda with a sensitivity test on decadal variability

It is advisable to refer to the publisher's version if you intend to cite from the work. See Guidance on citing.

To link to this article DOI: http://dx.doi.org/10.1007/978-3-031-08568-0_7

www.reading.ac.uk/centaur

CentAUR

Central Archive at the University of Reading

Reading's research outputs online

Chapter 7
Development of a Simple, Open-Source Hurricane Wind Risk Model for Bermuda with a Sensitivity Test on Decadal Variability

Pinelopi Loizou, Mark Guishard, Kevin Mayall, Pier Luigi Vidale, Kevin I. Hodges, and Silke Dierer

Abstract A hurricane-catastrophe model was developed for assessing risk associated with hurricane winds for Bermuda by combining observational knowledge with property value and exposure information. The sensitivity of hurricane wind risk to decadal variability of events was tested. The historical record of hurricanes passing within 185 km of Bermuda was created using IBTrACS. A representative exposure dataset of property values was developed by obtaining recent governmental Annual Rental Value data, while Miller et al. (Weather Forecast 28:159–174, 2013) provided a vulnerability relationship between increasing winds and damage. With a probabilistic approach, new events for 10,000 years were simulated for three different scenarios using (1) the complete record of annual TC counts; (2) two high-frequency periods and; (3) two low-frequency periods. Exceedance probability curves were constructed from event loss tables, focusing on aggregating annual losses from damaging events. Expected losses of low-frequency scenarios were less than losses of high-frequency scenarios or when the whole historical record was

P. Loizou (✉)
Department of Meteorology, University of Reading, Reading, UK
e-mail: pinelopi.loizou@pgr.reading.ac.uk

M. Guishard
Bermuda Weather Service, Bermuda Airport Authority, St. George's, Bermuda
e-mail: mguishard@airportauthority.bm

K. Mayall
Locus Ltd, Hamilton, Bermuda
e-mail: kmayall@locus.bm

P. L. Vidale · K. I. Hodges
National Centre for Atmospheric Science, Department of Meteorology, University of Reading, Reading, UK
e-mail: p.l.vidale@reading.ac.uk; k.i.hodges@reading.ac.uk

S. Dierer
Axis Capital, Zurich, Switzerland
e-mail: silke.dierer@axiscapital.com

used. This framework suffers from uncertainties due to different assumptions and biases within IBTrACS. Small data sizes limit our ability to conduct a formal model validation and results should be interpreted in this context. In the future, sensitivity tests on the different components of the model will be performed.

Keywords Hurricanes · Catastrophe modelling · Decadal variability

7.1 Introduction

Tropical cyclones (TCs) belong to the category of weather systems which bring severe damage and destruction across many regions of the planet in respect to rain, winds, and storm surge. Studies by McCarthy et al. (2015) and Goldenberg et al. (2001) have shown that TC activity around the globe undergoes important variability through the decades. Insurance and re-insurance companies can be particularly impacted by TCs, especially in countries that are more likely to see a TC making landfall.

Table 7.1 provides information about the ten costliest Atlantic hurricanes (NOAA 2020a; U.S. Bureau of Labor Statistics n.d.; Kishore et al. 2018). It can be seen that four of them occurred during the last Atlantic hurricane seasons (2017 and 2018) while nine of them occurred during the past 20 years. The columns indicate: name; year; maximum achieved intensity; total numbers of fatalities; total cost in billions of US dollars unadjusted for inflation; and adjusted total cost for 2017 in billions of US dollars. Deaths and damage costs refer to the total numbers of fatalities (direct and indirect) and damages across all the affected areas and countries. It should be highlighted that when thinking about damage and impact from a hazard, it is useful to use a metric of the affected area's wealth, for example the Gross Domestic Product (GDP). Hurricane Maria (2017) can be seen as a notable example: even though the total damage caused by the hurricane was around $91.6 bn, the impact on Dominica was way more significant than the impact on the United States. The damage after adjusting for inflation was 244% of Dominica's 2017 GDP. In addition, the

Table 7.1 Top 10 costliest Atlantic Hurricanes (as of 2019)

Name	Year	Category	Deaths	Cost (in bn)	Cost 2017 (in bn)
Katrina	2005	5	1200	$125	$164.9
Harvey	2017	4	68	$125	$129.5
Maria	2017	5	Estimates up to >8500	$91.6	≥$94.9
Irma	2017	5	47	$77.2	$66.5
Sandy	2012	3	233	$68.7	$76.3
Ike	2008	4	103	$38	$43.3
Wilma	2005	5	23	$27.4	$34.4
Andrew	1992	5	26	$27.3	$47.6
Ivan	2004	5	92	$26.1	$33.9
Michael	2018	5	74	$25.1	$25.1 (US)

uncertainty and large range of fatalities (particularly in Puerto Rico) caused by Hurricane Maria can be attributed to the fact that the assessment of deaths was difficult to perform and that many people died because of delays (or inability) in receiving medical care (Kishore et al. 2018).

Insurance and re-insurance companies often use catastrophe models to quantify the risk associated with hurricanes. A catastrophe model is used for assessing financial impacts of catastrophes, for estimating physical damages of properties, and assigning probabilities to the range of potential outcomes (RMS 2020). There are three main components: hazard (in this case, information about tropical cyclones), exposure (information about properties), and vulnerability (information about the damage a property can get). The goal of catastrophe modelling is to combine the three main components for the estimation of financial loss from hazards.

The aim of the study is to combine what is known from the historical hurricane record with information about property values, exposure, and vulnerability to develop a hurricane catastrophe risk model to assess the risk for Bermuda. It is worth noting that the intent of this study is not to rigorously reproduce the methodology of traditional catastrophe model development used by insurers and re-insurers. However, we use the conceptual process as a guide to develop our hurricane wind risk model. Figure 7.1 presents time series of annual numbers of tropical cyclones. The red line indicates the time series for the whole North Atlantic basin, while the black bars present the number of storms that came within 185 km (or 100 nm) of Bermuda. The historical record of hurricanes is created by using the International
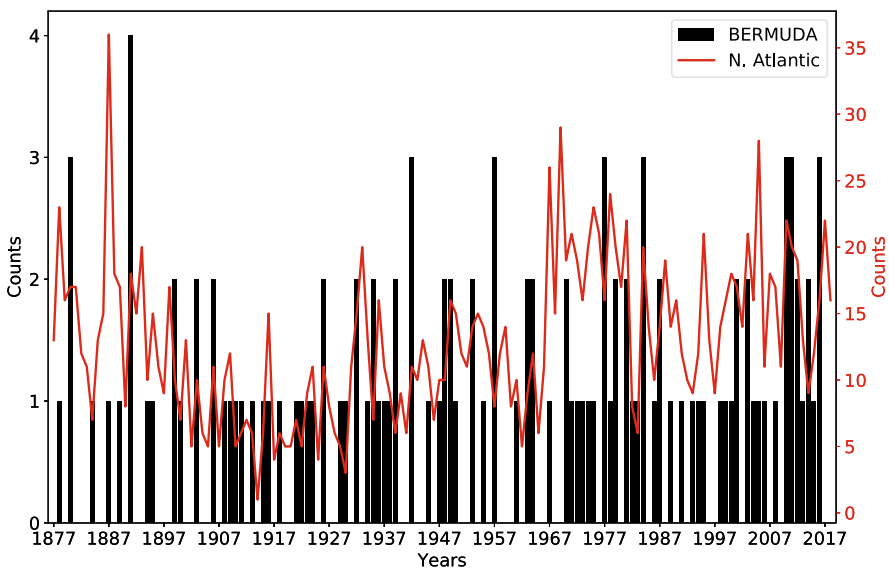

Fig. 7.1 Time series of annual numbers of tropical cyclones. Red line shows the time series for the whole North Atlantic basin. The black bars show the time series of storms that came within 185 km of Bermuda

Best-Track Archive for Climate Stewardship (IBTrACS) (Knapp et al. 2010). Recent Annual Rental Value data, taken from the Bermuda Government (2019), are used for the development of a representative dataset of property values for each of the 36 electoral constituencies in Bermuda. Miller et al. (2013) have performed damage analysis for Hurricane Fabian (2003) that shows the estimation of damage functions incorporating effects of topography. The study concluded that when topographic effects are taken into consideration for the near-surface wind speeds, there is a correlation between increasing damage and elevation.

7.2 Methodology

7.2.1 Data

For the purposes of this study, IBTrACS was used for obtaining a historical record for storms that have impacted Bermuda. In addition, Annual Rental Value data from the Bermuda Government are used for developing a representative dataset of property values for each of the 36 electoral constituencies in Bermuda.

7.2.1.1 Best-Track Dataset (Observations)

IBTrACS is a combination of the best track data taken from different agencies such as the Regional Specialized Meteorological Centers (RSMCs), the Tropical Cyclone Warning Centers (TCWCs), as well as other national agencies. The IBTrACS-ALL (v03r03) dataset, which includes data taken from all agencies, is used for this study. Full details can be found in Knapp et al. (2010). Data are available from 1877 until 2018. The agencies provide information about the best estimated position of each storm in terms of longitude and latitude in addition to reporting wind speed and mean sea level pressure (MSLP) values. The different agencies use different wind-averaging periods, and the values are reported in knots. The North Atlantic data are derived from the Hurricane Databases (HURDAT2) and are provided at 6-hour intervals. The wind speeds are 1-min sustained winds at 10 m, and they have been converted from knots to meters per second (multiplied by 1.94).

7.2.2 Exposure

7.2.2.1 Annual Rental Value Data

The Government of Bermuda's Land Valuation Department collects information about locations, types of property, size of living accommodation, size of any ancillary accommodation, amenities, and characteristics (Land Valuation

Table 7.2 Examples for the ARV data

2009 ARV	PV	Description	Address (fictional)	Parish
$15.600	780.000	APARTMENT	5 HARRY STREET HM01	CITY OF HAMILTON
$21.600	1.080.000	SHOP	8 HARRY STREET HM01	CITY OF HAMILTON
$13.800	690.000	APARTMENT	2 RONALD ROAD HM38	DEVONSHIRE
$33.600	1.680.000	HOUSE	8 FRED LANE MA12	SANDYS
$40.800	2.040.000	HOUSE	11 FLER LANE GE14	ST. GEORGE'S

Department 2019). They provide the Land Valuation List which includes location, type, and annual rental value (ARV) data. The ARV data used in this study are from 2009, but accessed in 2019, since more recent data were unavailable. A few representative examples of the ARV data are shown in Table 7.2. In order to protect the householders' personal information, the addresses displayed on the table are anonymized. The annual rental value is converted to estimated actual property value (PV) by multiplying by a factor of 50. In operational catastrophe models developed for re/insurance applications, building parameters such as construction type and number of stores are often used as second-order modifiers. In the case of the current analysis, secondary modifiers such as property type and location are available in the ARV dataset and could be used in future to refine and enhance this modelling framework.

7.2.3 Bermuda's Historical Record of Hurricanes

The first step of the process was to obtain a historical record of hurricanes that have either made landfall or that have been in close proximity to Bermuda. Therefore, by using the complete record for IBTrACS (1877–2018), for every year, for every storm, every track point which came within 185 km of Bermuda (32.39°N, 64.68°W) along with the wind speed information is kept for further analysis. The choice of 185 km is based on the threat parameter used by the Bermuda Weather Service (NOAA 2020a). The process is summarised on Fig. 7.2a. Figure 7.2b presents all the points that were kept for further analysis. Bermuda is indicated with a black cross.

For each point that is kept, the distance from Bermuda is calculated by using the Haversine formula given by:

$$d = r * c \tag{7.1}$$

where $r = 6371$ km is the Earth's radius and c is given by:

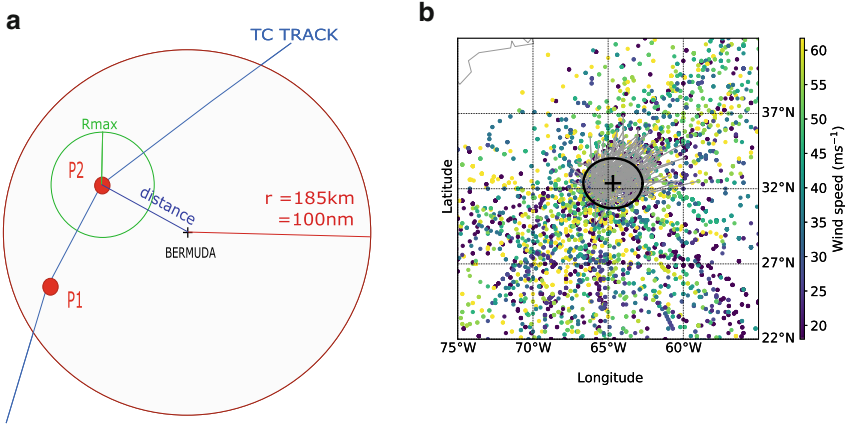$$c = 2 * \arctan\left(\frac{\sqrt{a}}{\sqrt{1-a}}\right) \tag{7.2}$$

Fig. 7.2 (**a**) Schematic of the methodology for creating the dataset of storms for Bermuda. (**b**) Tropical cyclones that passed within 185 km from Bermuda (black cross)

where

$$a = \sin^2\left(\frac{\phi_2 - \phi_1}{2}\right) + \cos(\phi_1) * \cos(\phi_2) * \sin^2\left(\frac{\lambda_2 - \lambda_1}{2}\right) \qquad (7.3)$$

with ϕ_1 and λ_1 the latitude and longitude coordinates of the storm track point in radians and ϕ_2 and λ_2 the latitude and longitude coordinates of Bermuda in radians. For each point, a radius of maximum wind (r_{max}) was chosen based on Eq. 7.4:

$$r_{max} = \begin{cases} 200 \text{ km}, v \leq 17 \text{ ms}^{-1} \\ 125 \text{ km}, 17 < v \leq 32 \text{ ms}^{-1} \\ 95 \text{ km}, 32 < v \leq 42 \text{ ms}^{-1} \\ 50 \text{ km}, 42 < v \leq 49 \text{ ms}^{-1} \\ 30 \text{ km}, 49 < v \leq 58 \text{ ms}^{-1} \\ 25 \text{ km}, 58 < v \leq 70 \text{ ms}^{-1} \\ 20 \text{ km}, v > 70 \text{ ms}^{-1} \end{cases} \qquad (7.4)$$

where v is the intensity from the IBTrACS. The values for r_{max} were chosen empirically based on a collection of data from H*WIND (NOAA 2020b) which included tropical cyclones that affected Bermuda during the period 2006–2014.

Then for each point that was saved, the intensity of the storm at Bermuda is calculated by:
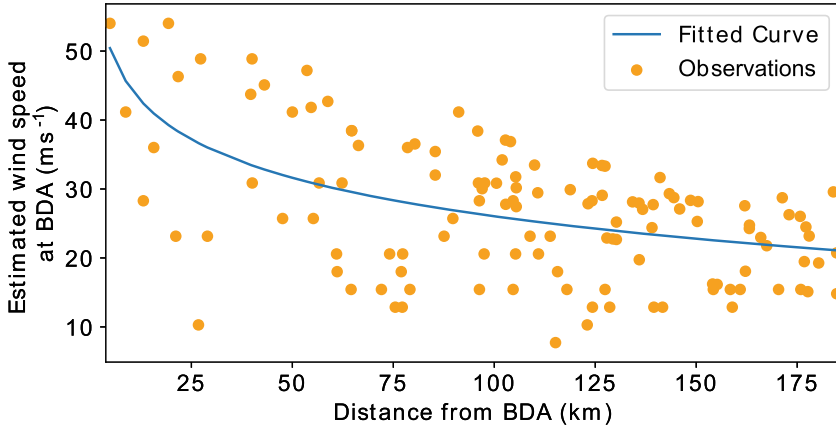
Fig. 7.3 Plot of estimated wind speeds at Bermuda against the distance from Bermuda (orange line). The blue line indicates a fitted logarithmic curve

$$v_{BDA} = \begin{cases} v * \sqrt{\dfrac{r_{max}}{d}}, & d > r_{max} \\ v, & d \leq r_{max} \end{cases} \tag{7.5}$$

where d is given by the aforementioned Haversine formula. The first part of Eq. (7.5) is a variation of the Rankine Vortex (Holland et al. 2010). Afterwards, for each year, for each storm, the point with the highest estimated intensity in Bermuda is retained. Eventually, all the points of the highest estimated intensities for all the storms that passed within 185 km of Bermuda are obtained. By sorting the data according to distance and fitting a logarithmic curve, a relationship between the distance of a storm from Bermuda and its estimated wind speed in Bermuda is obtained. The relationship is presented in Fig. 7.3 and it is described by:

$$f(x) = 63.1 - 8.05 * ln(x), \tag{7.6}$$

where x is the distance (d) in km and $f(x)$ is the wind speed in ms^{-1}.

A very important component of a catastrophe model is the relationship between wind and damage. According to Sealy and Strobl (2017) the appropriate way to simulate the relationship is by varying the damage of the property with the cubic power of the wind speed. For the purposes of this study, a damage index, f, proposed by Emanuel (2011) is used for the calculation of the proportion of damage as a function of wind speed, V:

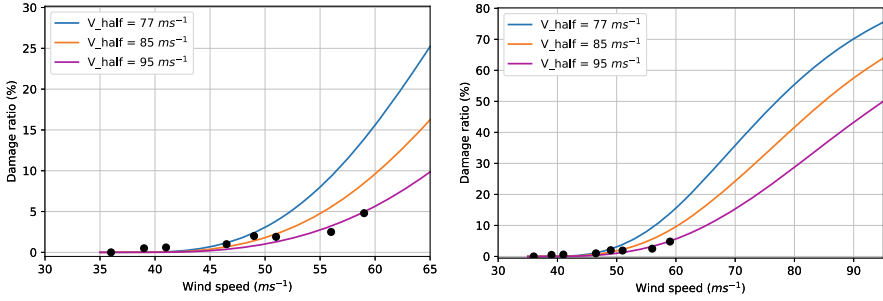$$f = \frac{u_i^3}{1 + u_i^3} \tag{7.7}$$

Fig. 7.4 Relationship between damage and wind speed. Black dots indicate an estimate of the Miller et al. (2013) figure 12 data. (**a**) Fitting the data with the different damage index curves by varying V_{half}; (**b**) projection of the different curves that were fitted to the data

where

$$u_i = \frac{MAX[(V_i - V_{thresh}), 0]}{V_{half} - V_{thresh}} \qquad (7.8)$$

where V_i is the estimated wind speed in Bermuda (calculated by Eq. 7.6), V_{thresh} is the wind speed below which no damage occurs, and V_{half} is the value of wind speed at which half of the property is damaged. Different studies (Emanuel 2011; Elliott et al. 2015; Sealy and Strobl 2017) have used a threshold of around 25.7 ms^{-1} (50 kts) for V_{thresh}, while for V_{half} different values were chosen based on the nature of each study. For this study, in order to choose appropriate thresholds, the data by Miller et al. (2013) were used. They found a threshold of approximately 37.5 ms^{-1} for the occurrence of roof damage. Therefore, by using $V_{thresh} = 37.5$ ms^{-1} and by varying V_{half} to best fit the Miller et al. (2013) data (see Fig. 7.4), it was found that at $V_{half} = 95$ ms^{-1} half of the property was damaged.

7.2.4 Generating New Datasets

The next step of the study involved using the historical record of annual number of storms for Bermuda shown in Fig. 7.1 to generate new random events with their potential losses. The process of generating new datasets, as summarized in Fig. 7.5, begins by calculating the probability of a number of hurricanes occurring. Previous studies (Jagger et al. 2001; Klotzbach 2010; Emanuel 2011; Scherb et al. 2015; Sealy and Strobl 2017) have suggested using the Poisson distribution since it provides a simple method for computing the probability of hurricane occurrence. The Poisson distribution is given by:

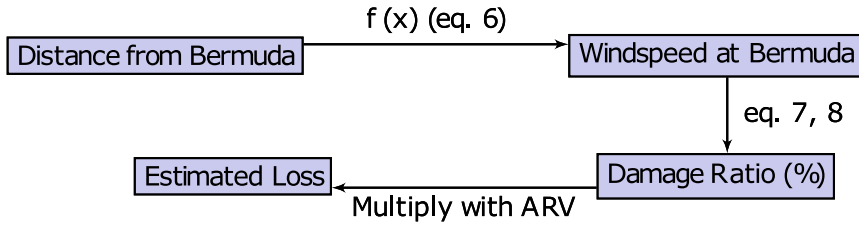$$P(X = k) = \frac{\lambda^k}{k!}e^{-\lambda} \qquad (7.9)$$

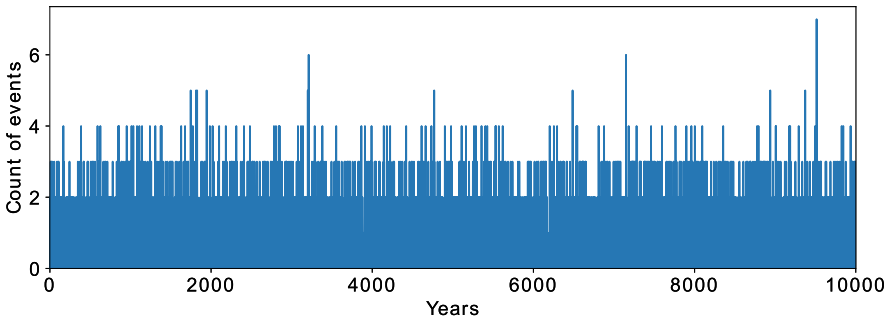**Fig. 7.5** Schematic of the process of generating the new datasets

Fig. 7.6 Time series of simulated events for 10,000 years

where λ is taken as the average annual number of hurricanes ($\mu = 0.86$) for Bermuda from the historical record. Afterwards, random events (Fig. 7.6) for the period of 10,000 years were generated from the Poisson distribution. To each event, a randomly generated number for distance (in km) between 0 and 185 was assigned. Then, by using Eqs. 7.6, 7.7, and 7.8, a wind speed and a damage ratio value are calculated and assigned to each event. Eventually, by using the PV data, the potential loss for each event can be estimated and then the sum of all the losses in each year is calculated.

7.2.5 Incorporating Decadal Variability

Numerous studies have shown that on decadal time scales, TC activity in the North Atlantic can be influenced by the Atlantic Multidecadal Oscillation (AMO) through variations of sea surface temperatures (Goldenberg et al. 2001; McCarthy et al. 2015; Ting et al. 2019; Murakami et al. 2020; Mann et al. 2021; Hallam et al. 2021). The associated warm and cold phases of the AMO can last for 20–40 years and they can lead, either directly or via modulation of other modes, such as the El-Niño Southern Oscillation (ENSO), to more or less active hurricane seasons (Knight 2005; Zhang and Delworth 2006; Klotzbach and Gray 2008). Therefore, the final step of the study
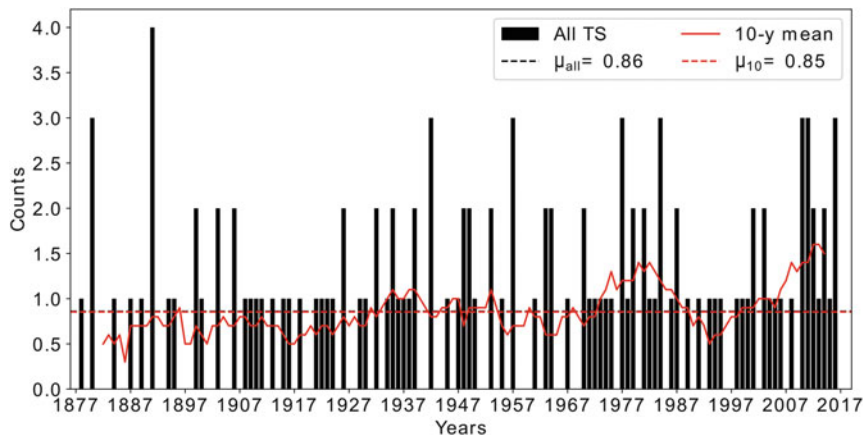
Fig. 7.7 Time series for Bermuda (black bars). The 10-year moving average is shown with the red solid line and its mean is shown with the dashed red line

was to test the model for different climate scenarios. To do that, different time periods with either increased or decreased TC activity within the time series were examined. The different periods were chosen based on the following steps:

1. Find the mean (μ_{all}) of the time series for the annual number of tropical storms in Bermuda.
2. Calculate the 10-year moving average of the time series (centred–red solid line in Fig. 7.7).
3. Find the mean of the 10-year moving average (μ_{10} – red dashed line in Fig. 7.7).
4. For high-frequency phases, take at least 10 consecutive years for which the 10-year moving average is greater than μ_{10} and the mean of the 10+ consecutive years to be greater than μ_{all}. Two high frequency phases were found: 1973–1989 and 1999–2014.
5. For low-frequency phases, take at least 10 consecutive years for which the 10-year moving average is less or equal than μ_{10} and the mean of the 10+ consecutive years to be less than μ_{all}. Two low-frequency phases were found: 1882–1895 and 1897–1930.

Then, for each phase, by using the mean of the phase, new events were randomly generated by following the process outlined in Sect. 7.2.4.

7.3 Results

The output of a catastrophe model is the loss amount from a catastrophic peril. This is given in the form of an Event Loss Table – the format and a data sample are shown in Table 7.3. By looking at the time series of simulated events on Fig. 7.6, the

Table 7.3 Example event loss table

Year	Event 1	Event 2	Event 3	Event 4	Event 5	Event 6	Event 7	Sum
0	14,512,670	–		–	–	–	–	14,512,670
1	0	–		–	–	–	–	0
2	0	0	–	–	–	–	–	0
3	0	0	0	10,238,454	–	–	–	10,238,454
4	0	0	0	0	–	–	–	0
5	45,319,873	–	–	–	–	–	–	45,319,873
6	0	8,749,651	45,319,873	–	–	–	–	54,069,523
7	–	–	–	–	–	–	–	0
8	13,099,546	14,512,670	–	–	–	–	–	27,612,216
9	16,005,999	0	–	–	–	–	–	16,005,999
10	0	10,238,454	–	–	–	–	–	10,238,454

maximum number of events in a single year in that scenario is seven individual events. Therefore, for Table 7.3 column 1 corresponds to the year number, columns 2–8 correspond to the losses from the individual events, and column 9 corresponds to the amount of loss in a year (the sum of losses from the individual events). It can be seen that there were years with no events (e.g., year 7), years with a single non-damaging event (e.g., year 1), years with a single damaging event (e.g., year 0), years with multiple non-damaging events (e.g., year 4), years with multiple damaging events (e.g., year 8), and years with both damaging and non-damaging events (e.g., year 3). From this tabulated output one can construct an Exceedance Probability (EP) curve. The EP curve describes the annual probability that an amount of loss will be exceeded. In constructing the EP curves, we focus on aggregating annual losses. If a more granular analysis were needed, effort would have been made to establish a specific identifier for each event. However, it is worth noting here that the model output has been constructed from an Aggregate Exceedance Probability (AEP) perspective and neglects further analysis of individual contributions to the annual losses (Occurrence Exceedance Probability - OEP). A future refinement would be to assess the variability of loss events on an annual basis via an OEP analysis.

Figure 7.8 presents the cumulative distribution function (CDF) of expected losses on all properties in all parishes of Bermuda when the whole time series of annual counts of tropical storms for Bermuda is used for simulating new events. The histogram (empirical results) indicates the actual losses from events that were intense enough to cause damage, meaning events that had an estimated wind speed at Bermuda greater than 37.5 ms^{-1} (based on Miller et al. 2013). The black dashed line indicates the theoretical CDF, meaning what one would expect to observe if there was an infinite number of damaging events. Non-damaging events were excluded from the analysis, but we present all the model output. For example, by
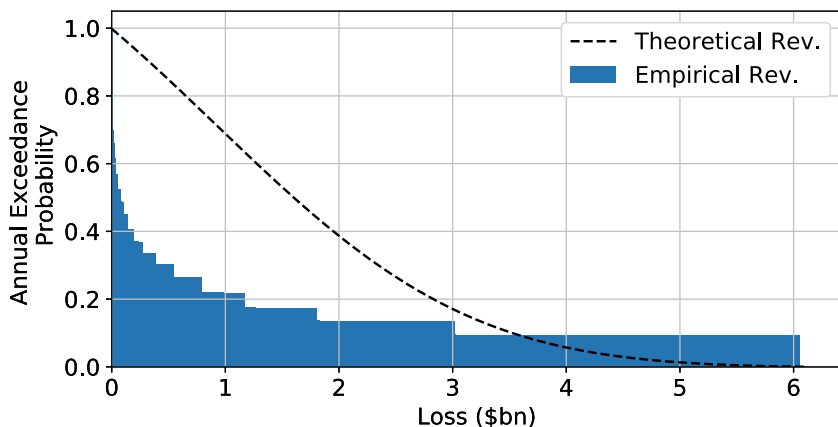

Fig. 7.8 Cumulative distribution function (CDF) of expected AEP losses on all properties, all parishes of Bermuda when the 1877–2018 record for Bermuda was used for simulating new events. The histogram indicates the empirical CDF of losses from damaging events

looking at the histogram from the empirical results, there is a 21.9% chance that during a year with at least one damaging event, losses will exceed $1bn.

Examination of the decadal variability of TCs revealed two high-frequency and two low-frequency phases. High-phases A and B correspond to the periods 1973–1989 (with mean $\mu = 1.18$) and 1999–2014 (with mean $\mu = 1.31$), respectively, during which the 10-year moving average was greater than the mean of the 10-year moving average. Low-phases A and B correspond to the periods 1882–1895 (with mean $\mu = 0.64$) and 1897–1930 (with mean $\mu = 0.68$), respectively, during which the 10-year moving average was less than or equal to the mean of the 10-year moving average.

For each one of the four phases, the mean was calculated and used as described in Sect. 7.2.4 to find the Poisson rate probability of number of events occurring, from which new events were randomly generated for each phase. Empirical and theoretical CDFs were plotted for each phase, as well as for the CDF shown in Fig. 7.8 (hereafter referred to as no-phase), and are shown in Fig. 7.9.

Results showed that losses from damaging events sampled from both high-frequency scenarios were larger than the losses from damaging events sampled from the two low-frequency scenarios and the no-phase scenario. In addition, the annual exceedance probabilities for low-phase B were smaller than the ones for low-phase A, while the probabilities for high-phase B were greater than the ones for high-phase A. It should be noted that, since the process of simulating new events is random, the output of the model will not always resemble the results presented here.

Furthermore, the number of simulated events is dependent on the average annual number of hurricanes. For this study, the means of the different phases ranged from 0.64 to 1.13 hurricanes per year. It is expected that a significantly higher annual
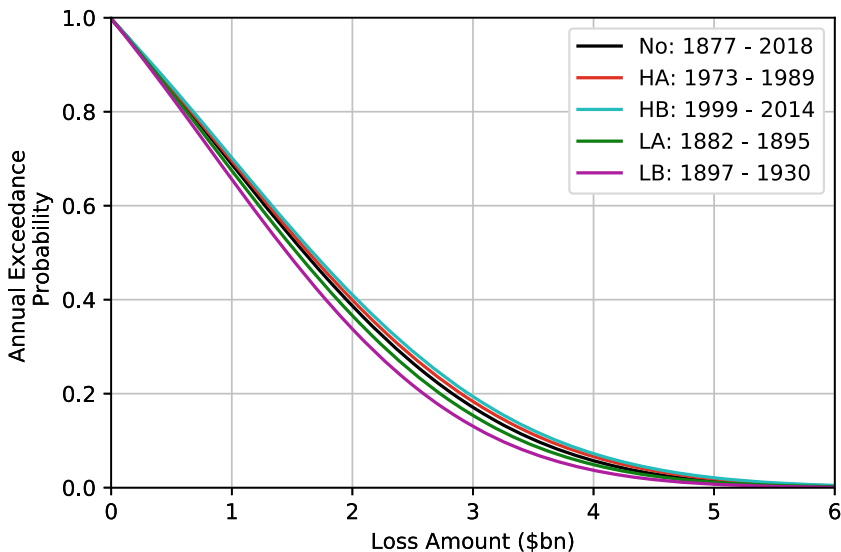

Fig. 7.9 EP curves for all five scenarios

average will result in a significantly increased number of simulated events, and thus larger losses. Lastly, it is important to highlight that, based on Eq. 7.6, the highest wind speed of a simulated event can be up to 63.1 ms^{-1}, while the lowest damaging wind speed is 37.5 ms^{-1}. It is certain that if the former value were higher or if the latter value were lower, the resulting EP curves would be very different, showing greater losses particularly in a high-frequency scenario. In future work, the sensitivity of the model on both the effect of the average annual rate of hurricanes and the estimated wind speed in Bermuda will be explored.

Information about return periods (RP) of catastrophic events can be obtained from EP curves. The return period (in years) corresponds to 1/EP. Table 7.4 presents examples of EP values and the corresponding RPs for all five scenarios shown in Fig. 7.9 for six different loss amounts. The loss amounts are shown in column 1, EPs and RPs for the no-phase scenario are in columns 2 and 3, for the two high-phase scenarios in columns 4–7 and for the two low-phase scenarios in columns 8–11. For example, in the no-phase scenario there is a 5.7% probability that an amount of $4bn will be exceeded in a year with at least one damaging event. This probability corresponds to a RP of around 17.5 years. The probability that the same amount will be exceeded rises for both high-frequency scenarios and dips for both low-frequency scenarios.

Table 7.5 presents examples of estimated losses for certain return periods of catastrophic events. The first and second columns indicate the return periods and

Table 7.4 Exceedance probability and return period values for different loss amounts

Loss	No-Phase		High-A		High-B		Low-A		Low-B	
	EP	RP	EP	RP	EP	RP	EP	RP	EP	RP
($bn)	(%)	(year)	(%)	(year)	(%)	(year)	(%)	(year)	(%)	(year)
0.50	84.8	1.2	85.2	1.2	85.5	1.2	84	1.2	83.1	1.2
1.00	68.9	1.5	69.3	1.4	70.1	1.4	67.4	1.5	65.7	1.5
2.00	38.7	2.6	40.0	2.5	41.2	2.4	36.7	2.7	33.7	3
3.00	17.1	5.8	18.3	5.5	19.4	5.2	15.4	6.5	13.1	7.6
4.00	5.7	17.8	6.6	15.3	7.2	13.9	4.9	20.6	3.7	27.2
5.00	1.3	75.9	1.8	54.5	2.1	47.4	1.2	86.6	0.7	138.5

Table 7.5 Loss amounts for different return period values

RP (years)	EP (%)	Loss ($bn)				
		No-Phase	High-A	High-B	Low-A	Low-B
5	20	2.8	2.9	3	2.7	2.6
10	10	3.5	3.6	3.7	3.4	3.2
25	4	4.3	4.4	4.5	4.1	3.9
50	2	4.7	4.9	5	4.6	4.4
75	1.3	5	5.2	5.3	4.9	4.7
100	1	5.2	5.4	5.5	5.1	4.8
200	0.5	5.5	5.8	6	5.5	5.2

corresponding exceedance probabilities, while expected losses for each scenario are shown in the remaining columns. For example, a once-in-200-years catastrophic event is expected to cause $5.5bn worth of damage across all parishes and all types of buildings in a no-phase scenario, compared to $6bn in a high-phase B scenario. These losses are halved for a catastrophic event with a return period of once-per-five-years.

Event Loss Tables and EP curves provide the ability to yield indicative return periods of threshold loss events (or changes in magnitude of losses for a given return period). This is very important for insurance and re-insurance companies since they are provided with necessary information that can help in the process of decision making.

7.4 Limitations and Future Work

This study serves as a simple catastrophe model for assessing annual hurricane wind risk in Bermuda, with a scientifically informed sensitivity test on long-term frequencies. It does not intend to reproduce traditional catastrophe modelling methodologies widely used by insurance and re-insurance companies, but to merely serve as a guide for the development of a hurricane wind risk model.

The process of building a catastrophe model entails various sources of uncertainties in all the different components.

Firstly, a key limitation of the study is the use of the observational record. Despite the fact that the record for the North Atlantic basin is considered to be the longest and most comprehensive record compared to other basins (Strachan et al. 2013), it suffers from homogeneity problems due to changes in operational procedures (Landsea 2007), whose most important source of uncertainty is the observational error (Tolwinski-Ward 2015). In addition, evaluation of the model with historical losses is problematic, as there are only a few very recent official reports from damaging storms affecting Bermuda that can be used for calibration purposes. So, not only are the basin-wide statistics a source of uncertainty, but the damaging impacts in Bermuda are also insufficient to affect a useful calibration of the model.

Secondly, different decisions made in the process of exploring the relationship between the distance of a storm from Bermuda and the estimated intensity in the country (see Sect. 7.2.3) is another source of uncertainty. These decisions include the arbitrary choices for r_{max}, the use of the variation of the Rankine vortex, the different conversions, and the curve fitting. In the future it would be really beneficial to explore different techniques for simulating hurricane intensity such as the ones outlined in Holland et al. (2010), Justus et al. (1978), and Jagger and Elsner (2006). In addition, wind asymmetries, the exclusion of which can have a negative impact on TC risk assessment (Pahwa 2007; Alvehag and Soder 2011), could be addressed following suggestions by studies such as Olfateh et al. (2017) and Chang et al. (2020).

Thirdly, it is important to highlight the lack of studies in Bermuda that explore the relationship between the intensity of a storm and the proportion of damage on properties. Since the vulnerability component of a catastrophe model is of great importance, there is a necessity for more studies like Miller et al. (2013) to be conducted in future catastrophic events, since they will provide an opportunity for updates and sensitivity tests on this model framework.

Lastly, the impact of decadal variability of TCs on potential losses has been examined only in terms on frequency. It will be of great interest to explore the impact in terms of intensity as well. The reasoning behind this comes from the fact that, particularly for the North Atlantic basin, it has been shown that even during low-activity hurricane seasons, very intense tropical cyclones can cause a lot of damage and destruction should they make landfall.

7.5 Discussion

We have developed a simple model for the assessment of hurricane wind risk. Despite the limitations of the study outlined above, this methodology may be useful for jurisdictions with limited availability of property exposure or vulnerability datasets. In the absence of a set of robust engineering studies or readily available property exposure data, assessments of the variability of risk can still be achieved, especially for small island jurisdictions. In our study, we utilized a real estate dataset and a published damage survey as the bases for development of exposure and vulnerability inputs, respectively. The hazard portion of this model is constructed by randomly generating multiple location-centric events that are constrained using the historical record. However, this approach is simple compared to the Monte Carlo simulations used to develop the stochastic storm track datasets in commercial catastrophe models (RMS 2019). Our method can quickly and easily be applied to assess the variability of wind hazard in different climate regimes, such as ENSO or the NAO, and can utilize other input such as historical anecdotal document archives (e.g. Chenoweth and Divine 2008), climate model simulations of future storm regimes (e.g. Wehner et al. 2015), or geological proxy datasets, such as those provided in Wallace et al. (2014). The simple nature of the model may also be of benefit in quick sensitivity tests of modelled losses to changes in hazard, vulnerability, or exposure. This may be especially useful for the purposes of teaching different aspects of risk and its estimation. The code underlying the model itself is written in Python, and it is accessible freely via Github here https://github.com/PinelopiLoizou/Risk_Model.

References

Alvehag K, Soder L (2011) A reliability model for distribution systems incorporating seasonal variations in severe weather. IEEE Trans Power Deliv 26:910–919. https://doi.org/10.1109/TPWRD.2010.2090363

Chang D, Amin S, Emanuel K (2020) Modeling and parameter estimation of hurricane wind fields with asymmetry. J Appl Meteorol Climatol 59:687–705. https://doi.org/10.1175/JAMC-D-19-0126.1

Chenoweth M, Divine D (2008) A document-based 318-year record of tropical cyclones in the Lesser Antilles, 1690-2007. Geochem Geophys Geosyst 9. https://doi.org/10.1029/2008GC002066

Elliott RJR, Strobl E, Sun P (2015) The local impact of typhoons on economic activity in China: a view from outer space. J Urban Econ 88:50–66. https://doi.org/10.1016/j.jue.2015.05.001

Emanuel K (2011) Global warming effects on U.S. hurricane damage. Weather Clim Soc 3:261–268. https://doi.org/10.1175/WCAS-D-11-00007.1

Goldenberg SB, Landsea CW, Mestas-Nuñez AM, Gray WM (2001) The recent increase in Atlantic hurricane activity: causes and implications. Science (80-) 293:474–479. https://doi.org/10.1126/science.1060040

Hallam S, Guishard M, Josey SA, Hyder P, Hirschi J (2021) Increasing tropical cyclone intensity and potential intensity in the subtropical Atlantic around Bermuda from an ocean heat content perspective 1955–2019. Environ Res Lett 16:034052. https://doi.org/10.1088/1748-9326/abe493

Holland GJ, Belanger JI, Fritz A (2010) A revised model for radial profiles of hurricane winds. Mon Weather Rev 138:4393–4401. https://doi.org/10.1175/2010mwr3317.1

Jagger TH, Elsner JB (2006) Climatology models for extreme hurricane winds near the United States. J Clim 19:3220–3236. https://doi.org/10.1175/JCLI3913.1

Jagger T, Elsner JB, Niu X (2001) A dynamic probability model of hurricane winds in coastal counties of the United States. J Appl Meteorol 40:853–863. https://doi.org/10.1175/1520-0450(2001)040<0853:ADPMOH>2.0.CO;2

Justus CG, Hargraves WR, Mikhail A, Graber D (1978) Methods for estimating wind speed frequency distributions. J Appl Meteorol 17(3):350–353

Kishore N et al (2018) Mortality in Puerto Rico after Hurricane Maria. N Engl J Med 379:162–170. https://doi.org/10.1056/NEJMsa1803972

Klotzbach P (2010) 3A.4 Caribbean/Central American hurricane landfall probabilities

Klotzbach PJ, Gray WM (2008) Multidecadal variability in North Atlantic tropical cyclone activity. J Clim 21:3929–3935. https://doi.org/10.1175/2008JCLI2162.1

Knapp KR, Levinson DH, Kruk MC, Howard JH, Kossin JP (2010) The International Best Track Archive for Climate Stewardship (IBTrACS) project: overview of methods and Indian ocean statistics. Indian Ocean Trop Cyclones Clim Chang 215–221. https://doi.org/10.1007/978-90-481-3109-9_26

Knight JR (2005) A signature of persistent natural thermohaline circulation cycles in observed climate. Geophys Res Lett 32:L20708. https://doi.org/10.1029/2005GL024233

Land Valuation Department (2019) Bermuda government - land valuation department. https://www.landvaluation.bm/. Accessed 1 July 2019

Landsea C (2007) Counting Atlantic tropical cyclones back to 1900. EOS Trans Am Geophys Union 88:197–202. https://doi.org/10.1029/2007EO180001

Mann ME, Steinman BA, Brouillette DJ, Miller SK (2021) Multidecadal climate oscillations during the past millennium driven by volcanic forcing. Science (80-) 371:1014–1019. https://doi.org/10.1126/science.abc5810

McCarthy GD, Haigh ID, Hirschi JJM, Grist JP, Smeed DA (2015) Ocean impact on decadal Atlantic climate variability revealed by sea-level observations. Nature 521:508–510. https://doi.org/10.1038/nature14491

Miller C, Gibbons M, Beatty K, Boissonnade A (2013) Topographic speed-up effects and observed roof damage on Bermuda following Hurricane Fabian (2003). Weather Forecast 28:159–174. https://doi.org/10.1175/waf-d-12-00050.1

Murakami H, Delworth TL, Cooke WF, Zhao M, Xiang B, Hsu P-C (2020) Detected climatic change in global distribution of tropical cyclones. Proc Natl Acad Sci 117:10706–10714. https://doi.org/10.1073/pnas.1922500117

NOAA (2020a) Costliest U. S. tropical cyclones. NOAA Tech Memo NWS NHC-6:1–5

NOAA (2020b) H*WIND-Real-time hurricane analysis project. https://storm.aoml.noaa.gov/hwind/. Accessed 10 July 2019

Olfateh M, Callaghan DP, Nielsen P, Baldock TE (2017) Tropical cyclone wind field asymmetry-development and evaluation of a new parametric model. J Geophys Res Ocean 122:458–469. https://doi.org/10.1002/2016JC012237

Pahwa A (2007) Modeling weather-related failures of overhead distribution lines. In: 2007 IEEE Power Engineering Society general meeting, vol. 21 of, IEEE, 1–1

RMS (2019) About us https://www.rms.com/catastrophe-modeling

RMS (2020). Understanding catastrophe. https://www.rms.com/catastrophe-modeling. Accessed 26 Jan 2021

Scherb A, Garrè L, Straub D (2015) Probabilistic risk assessment of infrastructure networks subjected to hurricanes. 12th Int Conf Appl Stat Probab Civ Eng ICASP 2015:1–9

Sealy KS, Strobl E (2017) A hurricane loss risk assessment of coastal properties in the caribbean: evidence from the Bahamas. Ocean Coast Manag 149:42–51. https://doi.org/10.1016/j.ocecoaman.2017.09.013

Strachan J, Vidale PL, Hodges K, Roberts M, Demory ME (2013) Investigating global tropical cyclone activity with a hierarchy of AGCMs: the role of model resolution. J Clim. https://doi.org/10.1175/JCLI-D-12-00012.1

Ting M, Kossin JP, Camargo SJ, Li C (2019) Past and future hurricane intensity change along the U.S. East Coast. Sci Rep 9:7795. https://doi.org/10.1038/s41598-019-44252-w

Tolwinski-Ward SE (2015) Uncertainty quantification for a climatology of the frequency and spatial distribution of North Atlantic tropical cyclone landfalls. J Adv Model Earth Syst 7:305–319. https://doi.org/10.1002/2014MS000407

U.S. Bureau of Labor Statistics (n.d.) CPI inflation calculator. https://data.bls.gov/cgi-bin/cpicalc.pl. Accessed 7 July 2019

Wallace DJ, Woodruff JD, Anderson JB, Donnelly JP (2014) Palaeohurricane reconstructions from sedimentary archives along the Gulf of Mexico, Caribbean Sea and western North Atlantic Ocean margins. Geol Soc London Spec Publ 388:481–501. https://doi.org/10.1144/SP388.12

Wehner M, Prabhat KAR, Stone D, Collins WD, Bacmeister J (2015) Resolution dependence of future tropical cyclone projections of CAM5.1 in the U.S. CLIVAR hurricane working group idealized configurations. J Clim 28:3905–3925. https://doi.org/10.1175/jcli-d-14-00311.1

Zhang R, Delworth TL (2006) Impact of Atlantic multidecadal oscillations on India/Sahel rainfall and Atlantic hurricanes. Geophys Res Lett 33:L17712. https://doi.org/10.1029/2006GL026267